 doi:10.20944/preprints202107.0587.v1

Article

2D-heterostructure Photonic crystal formation for on-chip polarization division multiplexing

Nikolay Lvovich Kazanskiy [1, 2], Muhammad Ali Butt [1, 3,*] and Svetlana Nikolaevna Khonina [1, 2]

[1] Samara National Research University, 443086 Samara, Russia; butt.m@ssau.ru
[2] Institute of RAS-Branch of the FSRC "Crystallography and Photonics" RAS, 443086 Samara, Russia; kazanskiy@ipsiras.ru (N.L.K); khonina@ipsiras.ru (S.N.K)
[3] Warsaw University of Technology, Institute of Microelectronics and Optoelectronics, Koszykowa 75, 00-662 Warszawa, Poland
* Correspondence: butt.m@ssau.ru

Abstract: Herein, we offer a numerical study on the devising of a unique 2D-heterostructure Photonic crystal (PC) that can split two orthogonally polarized light waves. The analysis is performed via a two-dimensional finite element method (2D-FEM) by utilizing COMSOL Multiphysics software. The device consists of two discrete designs of PC formation. The first PC formation is optimized so that it permits both TE and TM-polarization of light to transmit through it. Whereas the second PC formation possesses a Photonic Bandgap (PBG) only for TE-polarized light. These two formations are combined at an angle of 45 degrees, resulting in a reflection of self-collimated TE-polarized light at an angle of 90 degrees owing to the PBG present in the second PC formation. While permitting the self-collimated TM-polarized light wave to travel uninterrupted. The proposed device has a small footprint of ~10.9 μm^2 offering low transmission loss and high polarization extinction ratio which makes it an ideal candidate to be employed as an on-chip polarization division multiplexing system.

Keywords: Photonic crystal; polarizer; multiplexer; polarization extinction ratio; communication channels; heterostructure.

1. Introduction

In 1987, Yablonovitch [1] and John [2] suggested Photonic crystals (PCs), an artificial dielectric structure that uses periodic and random variations in the refractive index to maneuver the light flow. On a microscopic scale, it is possible to customize the propagation of the electromagnetic (EM) field in these constructions. Within the PC, EM waves scatter, and destructive interference occurs at specific wavelengths, forming a photonic bandgap (PBG) like the energy bandgap of electron waves in a semiconductor [3]. Controlling light propagation may be feasible due to the possibility of generating a PBG. Furthermore, devices with tiny footprints are possible. These remarkable characteristics might have an advantage to the development of compact integrated circuits. PCs are utilized in several notable applications such as polarizers [3-6], power splitter [7,8], solar cell [9], logic gates [10, 11, 12], optical diode [13], laser [14], sensor [15] and self-collimation [16, 17], among others. For a detailed study on PC applications, we suggest a timely review to the readers [18].

Multiplexing is a promising resolution in response to the enduring demand for increased transmission capacity [19-24]. Silicon (Si)-based photonic integrated circuits (PICs) may be utilized in data centers, high-performance computing, and optical communication networks because they are well-suited with CMOS technology, which allows for large-scale and cost-effective integration [25, 26]. Multi-dimensional multiplexing technologies, such as wavelength division multiplexing (WDM)[27], polarization division

multiplexing (PDM) [28], mode division multiplexing (MDM)[29], and others have gathered a lot of consideration in research and practical applications to expand interconnection or communication capacity. PDM is one of them, having the potential to double the transmission capacity and the capability to be linked with other multiplexing or advanced modulation format technologies, supporting its widespread use in commercially available optical communication systems. On the Si-based technology, numerous polarization-handling modules or PDM signal-processing devices have been effectively implemented [30-32]. The benefit of PDM is that the communication capacity is increased since separate signals can be dispersed over orthogonal states of polarization of the same light [33]. The two polarization channels are isolated at the receiver end and are individually identified. In an ideal world, at each end of the fiber link, the only requirement is to install a transceiver and a related polarization MUX/DEMUX, while the remaining network remains unaffected.

Dielectric waveguides (WGs) are often larger because they involve a large radius of curvature to prevent severe bending loss [34]. Optical WGs established on the PC formation vary from typical WGs in that they provide vigorous optical confinement as well as adaptable light-guiding [35-37]. The propagation of an EM wave via a steep bend with minimum bending loss is one of the remarkable uses of PC WGs [36]. This promotes the development and production of PC-based WGs. However, significant bending loss arises due to reflections at the acute bending corner, particularly when the bending angle is bigger than 90°. Subsequently, a significant study has been performed on the enhancement of bends to reduce reflection loss [38,39].

Usually, PC-WG structures are utilized to create polarization filters which makes them unattractive in the scenarios where polarization splitting is desired. A compact TM-mode pass filter created on a rectangular-air hole 1D-PC WG is proposed which delivers a polarization extinction ratio (PER) of >30 dB [40]. In [41], the PC-WG polarizer is numerically investigated by engineering the defect modes in the PBG structures. However, the device works as a polarization-maintaining device where one polarization can be completely blocked based on the radius of the defect rods. In [6], a T-shaped PBS based on 2D PC is proposed which is composed of three WGs offering a PER of 30 dB for both modes. PBSs based on resonant-coupling mechanism has also been reported in the past which offers good device performance. However, the design configuration is complicated which makes it difficult to implement the device without avoiding fabrication errors [5,42]. Moreover, a TM-polarization pass filter realized on a subwavelength grating WG has been demonstrated with PER of ~ 27 dB over a device length of 9 μm [43].

In this paper, we presented a 2D-PC heterostructure based on a SOI platform for polarization beam splitting application. Two PCs, known as PC-1 and PC-2 formations with different optical properties are joined at 45° so that light with TE-polarization is reflected at the boundary between PC-1 and PC-2 formation while self-collimated light having TM-polarization can travel without suffering from diffraction. By employing such a trait, a polarization beam splitter (PBS) is realized which can be employed as an on-chip PDM system. The proposed device is compact with a single interface between the two PC formations. This fact facilitates the fabrication process without significant errors due to its simple lattice structure. Moreover, the optimized PC formation allows the propagation of a collimated TE and TM-polarized light without forming any WG arrangement. The simulations are conducted via 2D-FEM where the geometry of the PC formation is adjusted to achieve the best performance. The “electromagnetic waves frequency domain (emw)” is employed as the physics interface and the “frequency domain” was included in the study. The sub-domains in the PC formation are split into triangular mesh elements with a “Physics-controlled mesh”. The meshing is based on the processing power of the system used. We picked a “fine mesh” size that gives realistic solutions established on our system’s processing speed. Scattering boundary conditions (SBCs) are assigned to the simulation window’s outer borders.

Preprints (www.preprints.org) | NOT PEER-REVIEWED | Posted: 26 July 2021 doi:10.20944/preprints202107.0587.v1

2. Modelling of PC-1 formation

The first PC formation is denoted as PC-1 which is constituted of a regular assortment of circular air holes etched in the silicon-on-insulator (SOI) platform as exhibited in figure 1a. The lattice constant and radius of the air hole is represented as *a* and *R*, respectively. Where *a* is the center-to-center gap between two air holes. The PC-1 formation is tailored to produce a homogeneous media where light having TE, and TM-polarization can travel through PC-1 devoid of any PBG. The TE and TM-polarized plane waves of width 2 μm are connected at the input port (P1) of the PC formation while the output is gathered at the output port (P2). The subsequent formula can be used to determine the transmission loss (*TL*):

$$TL\ (dB) = 10 \times log\left(\frac{P_{out}}{P_{in}}\right)$$

Where P_{out} and P_{in} are the output and input power, respectively which is obtained by utilizing the line integration built-in function in COMSOL Multiphysics software. The *TL* of TE and TM-polarized light at the operational wavelength=1550 nm is plotted for the lattice constant *(a)* ranging between 400 nm and 450 nm as shown in figure 1b. Five different values of radius (*R*) of the circular air hole is selected, i.e., *R*=0.25*a*, *R*=0.3*a*, *R*=0.35*a*, *R*=0.4*a* and *R*=0.45*a*. The selection of the geometric parameters is based on the operating wavelength and the ease of precisely fabricating the PC formations. *R* should always be smaller than *a*, otherwise, two air holes can overlap each other, and the device will not work efficiently as desired. The values *R*=0.4*a* and *R*=0.45*a* must be avoided as TE-polarized light suffer heavy *TL* due to scattering or the presence of PBG. The *TL* of <0.79 dB is acquired for both the polarization at the optimum value of *a*=420 nm and *R*=0.35*a*.

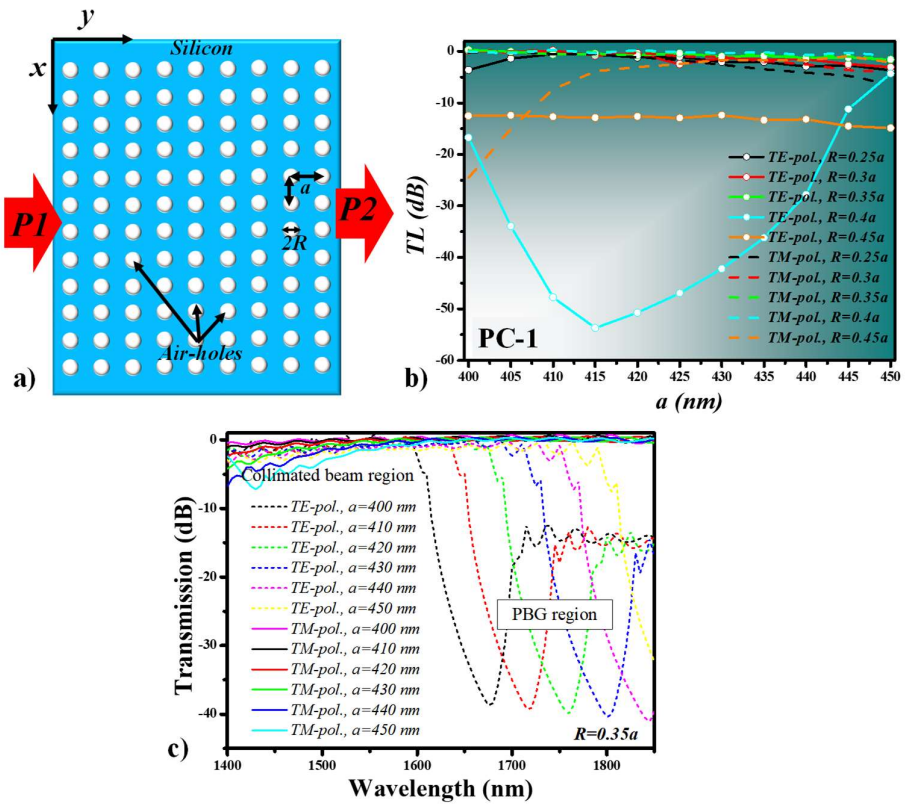

Figure 1. a) Graphical representation of PC-1 formation, b) The *TL* of TE and TM-polarized light travelling in PC-1 formation at 1550 nm. c) Transmission of TE and TM-polarized light for the wavelength range of 1400 nm to 1850 nm.

The PC-1 formation is analyzed for the determination of the collimation beam region and PBG region in the wavelength range of 1400 nm to 1850 nm. The geometric parameters

Preprints (www.preprints.org) | NOT PEER-REVIEWED | Posted: 26 July 2021 doi:10.20944/preprints202107.0587.v1

variables such as R is fixed at 0.35a whereas a is varied between 400 nm and 450 nm. The transmission spectrum for TE and TM-polarized light in PC-1 is shown in figure 1c. There is no TM-PBG for the whole wavelength range, however, at a>420 nm, the light is not collimated anymore. For TE-polarized light, there exists a strong PBG which depends on the lattice constant (a) of the PC-1. Therefore, the selection of geometric parameters should be wisely adapted for the wavelength range of interest. To visualize the propagation of light in PC-1 formation, the normalized electric field mapping of TE and TM-polarized light at λ=1550 nm is represented as shown in figure 2a and figure 2b, respectively. The structural variables such as a and R of the PC-1 are fixed at 420 nm and 0.35a, respectively. The PC-1 formation is capable of propagating self-collimated TE and TM-polarized light which indicates that there is no PBG in the designed PC-1 formation.

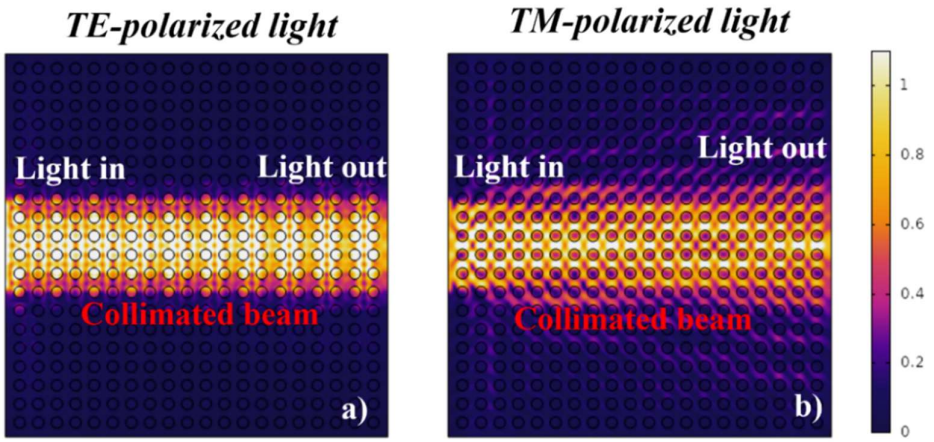

Figure 2. Norm. electric field distribution at λ=1550 nm at, a) TE-polarization of light, b) TM-polarization of light.

3. Modelling of PC-2 formation

The PC-2 formation is tailored such that there exists a PBG for TE-polarization of light, whereas TM-polarized light let go freely within the formation. It is comprised of a periodic collection of square air holes etched in the SOI platform as exhibited in figure 3a. The side length of the air hole is represented as w. The structure variables of the PC-2 formation are adjusted to create a TE-PBG but agrees on the self-collimated TM-polarized light to propagate in PC-2 deprived of any significant TL. The TL of TE and TM-polarized light at the operational wavelength=1550 nm is plotted for the lattice constant (a) ranging between 400 nm and 450 nm as shown in figure 3b. Four different values of side length (w) of the square air hole are selected, i.e., w=0.5a, w=0.6a, w=0.7a and w=0.8a. From the figure, it can be seen that the PC-2 formation permits both polarizations to travel through it for w=0.5a and w=0.6a. At w=0.8a, there exist a weak TE-PBG which offers a TL=~14-15 dB. However, a strong TE-PBG occurs at w=0.7a which is evident in figure 3b. The TL of ~ 60 dB and ~ 0.1 dB is obtained for TE and TM-polarized light at a=420 nm and w=0.7a.

Preprints (www.preprints.org) | NOT PEER-REVIEWED | Posted: 26 July 2021 doi:10.20944/preprints202107.0587.v1

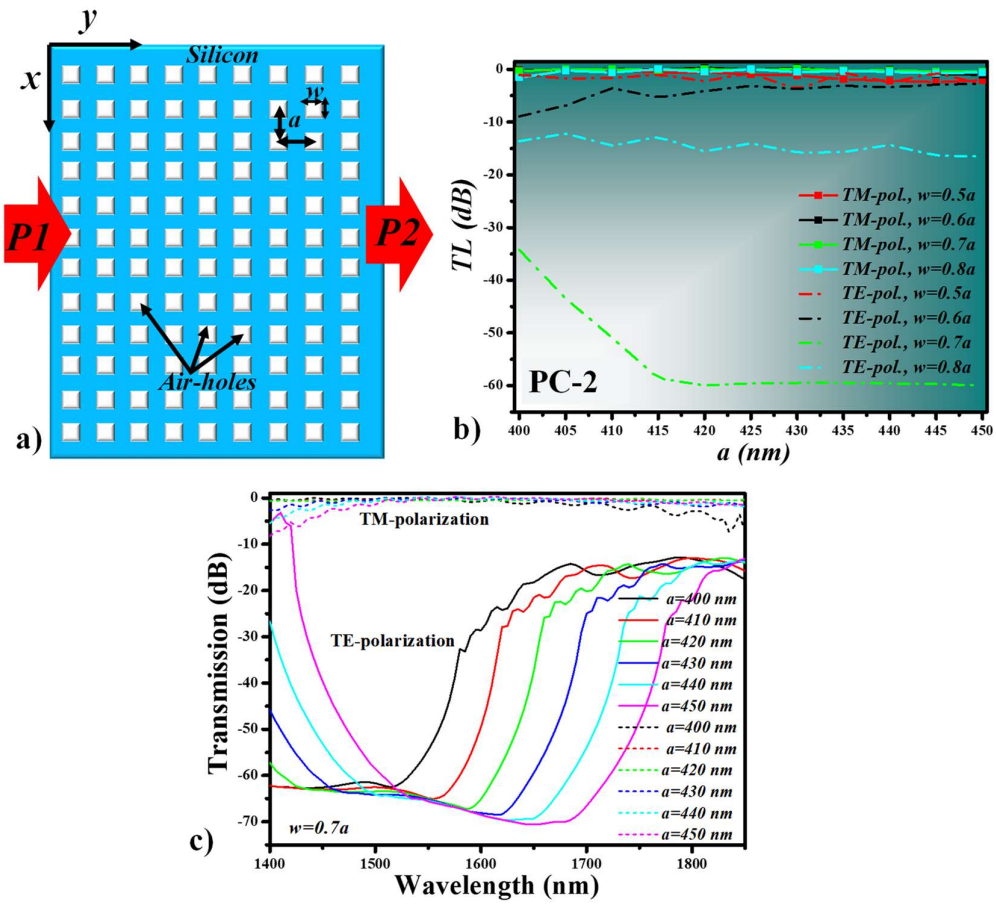

Figure 3. a) Graphical representation of PC-2 formation, b) The *TL* of TE and TM-polarized light travelling in PC-2 formation at λ=1550 nm, c) Transmission of TE and TM-polarized light for the wavelength range of 1400 nm to 1850 nm.

The PC-2 formation is studied to resolve the collimation beam region and PBG region in the wavelength range of 1400 nm to 1850 nm. The geometric parameters variables such as w is fixed at $0.7a$ whereas a is varied between 400 nm and 450 nm. The transmission spectrum for TE and TM-polarized light in PC-2 is presented in figure 3c. There is no TM-PBG for the whole wavelength range, however, at a>420 nm, the light is not collimated anymore. For TE-polarized light, there exists a strong PBG that begins at 1400 nm and extends to 1700 nm depending on the selection of a. We aim to design PC-2 in such a way that there exist a TE-PBG for the S, C and L telecommunication bands so that the device can help split the polarization in a heterostructure arrangement. The norm. electric field mapping of TE and TM-polarized light at λ=1550 nm is presented in figure 4a and figure 4b, respectively. When TE-polarized light is incident on the PC-2 formation, there exists a TE-PBG which blocks the light at the input. However, self-collimated TM-polarized light propagates diffraction-free from P1 and exits the formation from P2. This signifies the creation of a TM-polarizer formation that can be individually utilized in TM-polarization maintaining applications.

Preprints (www.preprints.org) | NOT PEER-REVIEWED | Posted: 26 July 2021 doi:10.20944/preprints202107.0587.v1

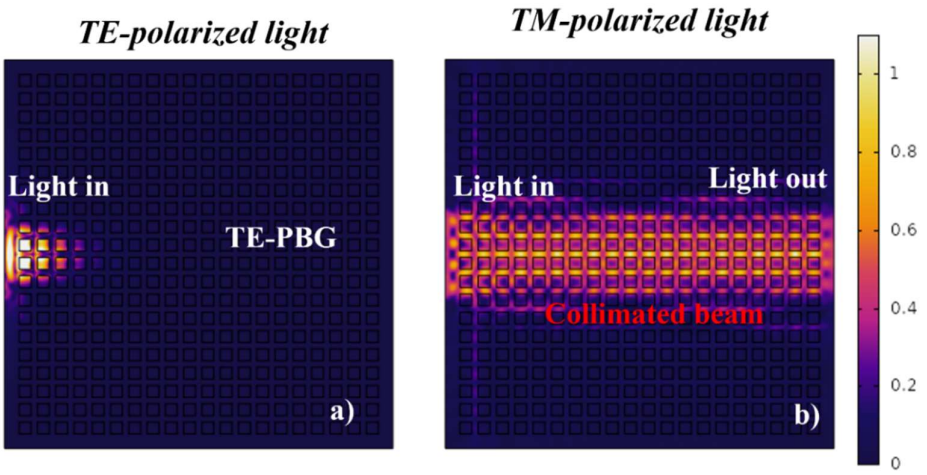

Figure 4. Norm. E-field mapping at λ=1550 nm at, a) TE-polarization of light, b) TM-polarization of light.

4. Polarization division multiplexing system

For the PDM system, the two optimized PC formations should be combined such that TE and TM polarization of light can split at 90°. The marriage of PC-1 and PC-2 in a distinctive way leads to the formation of PBS which can be employed as an on-chip PDM system. Both formations are combined at an angle of 45 degrees as shown in figure 5. The optimized values for PC-1 and PC-2 are adopted from the previous analysis where the *TL* is low and light travels without diffraction. For that purpose, we have used a=420 nm, R=0.35a and w=0.7a for PC-1 and PC-2. When the incident light (TE/TM) travelling from P1 passes the PC-1 and strikes the interface between PC-1 and PC-2, the TM-polarized light can continue its path and exit at P2. As both the formations act as a homogeneous medium and permit the self-collimated TM-polarized light to travel diffraction-free. While TE-polarized light reflects from the interface because of the presence of PBG in PC-2 and experiences a 90-degree bend. Consequently, a compact on-chip element is constructed which can be utilized in the PDM system to upsurge the number of transmission channels. The footprint of the device studied in this work is ~10.9 μm² because of 13 air-holes are periodically arranged in xy-plane having a=420 nm.

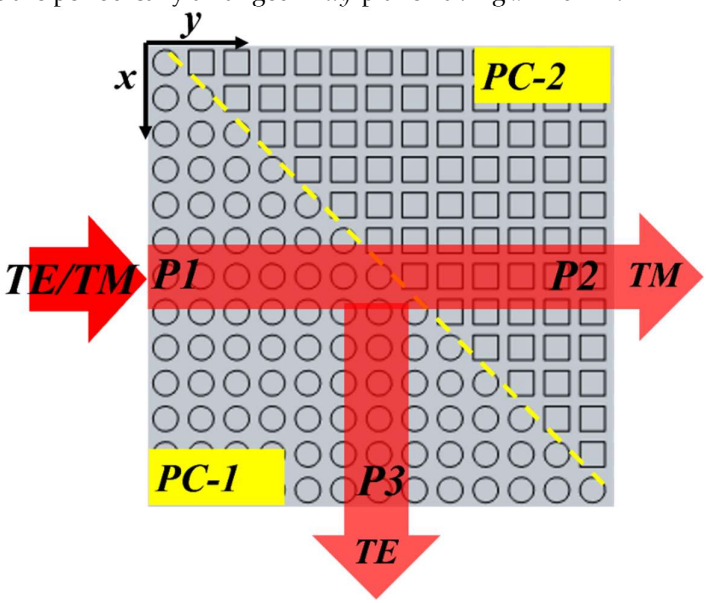

Figure 5. Graphical representation of heterostructure PC on-chip PMD.

Preprints (www.preprints.org) | NOT PEER-REVIEWED | Posted: 26 July 2021 doi:10.20944/preprints202107.0587.v1

The employment of the proposed device is easy where an unpolarized light can be coupled at the input port and the device splits the light into two orthogonal polarized lights. The orthogonal states of polarization (SOP) of the same light can be used for data transmission resulting in an expansion in the transmission capacity. The polarization multiplexing approach may be explained by comparing it to microwave communication systems. When two orthogonally polarized radio frequency signals are sent through wireless connections, the operator bandwidth can be increased. Two antennas with distinct polarization and orientation are utilized at the receiver to distinguish the signals. In optical systems, the two orthogonal SOP are detected at the receiver, letting each of the modulated signals be acquired separately.

The norm. electric field mapping of TE, TM, and TE+TM-polarized light at 1550 nm is shown in figure 6. It is evident that when the light having TE-polarization is given at the input (P1), the self-collimated TE-polarized light propagates in PC-1and reflects at 90 degrees after colliding with PC-2 eventually collected at P3 as shown in figure 6a. Self-collimated polarized light travels throughout both the formations and is collected at P2 as shown in figure 6b. If TE+TM polarized light is launched from P1, TE-polarized light is bent downward and collected at P3, while TM-polarized light travels straight and received at P2 as shown in figure 6c. This gives rise to the opportunity of utilizing this formation for a compact on-chip PDM scheme.

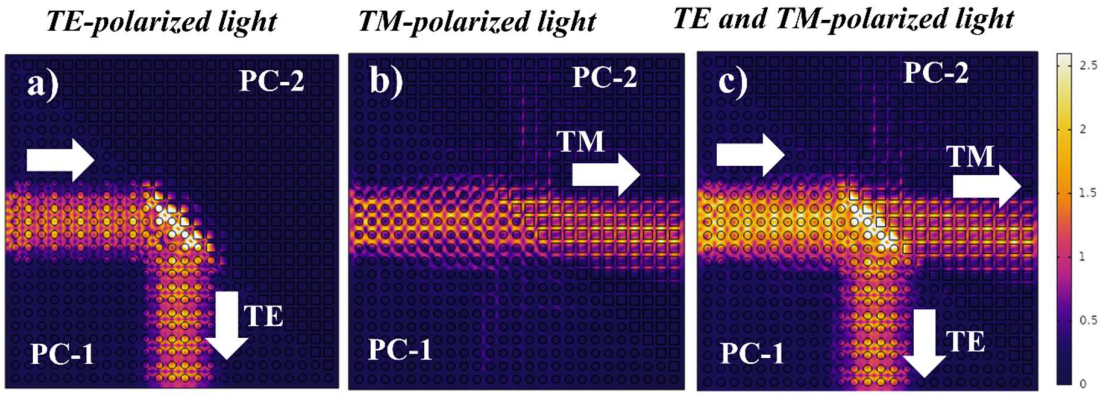

Figure 6. Norm. electric field mapping at λ=1550 nm for, a) light with TE-polarization, b) light with TM-polarization, c) TE+TM-polarization of light.

5. Results and discussion

PBS is a more challenging device than a polarizer since it must work equally effectively for both TE and TM polarized light. The transmission coefficient for both polarization outputs, which should be as near to unity as feasible, and cross talk and back reflection, which should be as low as possible, are the most important factors to evaluate. We used only one interface, as opposed to the PBS formation described in [44], which may minimize back-reflected light and increase transmissivity. PBSs based on PC heterostructures are worth investigating further. Polarization extinction ratio (PER) is an essential figure of merit that ought to be taken care of while devising the PBS formation. The power

Preprints (www.preprints.org) | NOT PEER-REVIEWED | Posted: 26 July 2021 doi:10.20944/preprints202107.0587.v1

of a specific polarization in the predicted output port versus the power of the same polarization in the other output port is defined as PER. Because it's a logarithmic ratio, the unit is in decibels which can be established for TE and TM-polarized light by utilizing the following formula: $PER_{P2}\ (dB) = 10log_{10}\left(\frac{P_{TM}}{P_{TE}}\right)$ and $PER_{P3}\ (dB) = 10log_{10}\left(\frac{P_{TE}}{P_{TM}}\right)$, respectively. Where PTM and PTE are the output power of the light having TM-polarization and the light having TE-polarization, respectively.

The TL and PER for the 2D-heterostructure PC are calculated for S, C and L telecommunication bands as shown in figure 7. The TL for the whole wavelength spectrum is in the range of 1.57 dB-3.5 dB and 0.25 dB-2 dB for TE and TM-polarized light, respectively. This includes the bending loss suffered by TE-polarized light. The PER calculated at P2 is significantly higher than the one obtained at P3. This is because TE-polarized light is entirely reflected from the interface which gives a pure TM polarized light at P2. The major portion of the TM-polarized light travels to P2 while some part of it reflects at the interface and enters the P3 which reduces the PER at P3. The maximum PER for 1550 nm obtained at P2 and P3 is ~40.5 dB and ~6.5 dB, respectively.

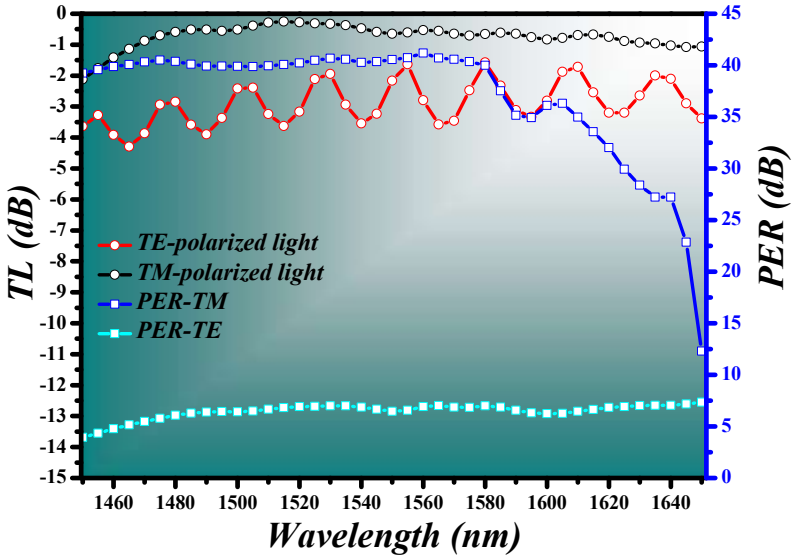

Figure 7. *TL* and *PER* of heterostructure PC.

6. Conclusions

In conclusion, a compact polarization beam splitter (PBS) device is numerically investigated by utilizing 2D-heterostructure Photonic crystals (PCs). The PC formations are designed in a unique way in which PC-1 allows the transfer of self-collimated TE and TM polarization of light. PC-2 is constructed such that there exists a photonic band bap (PBG) for TE-polarized light, however, TM-polarized light can travel devoid of any interference. These two distinctive PC formations are combined at an angle of 45 degrees which reflects the self-collimated TE-polarized light at 90 degrees sharp bend when it interferes with the PC-2 while allowing the self-collimated TM-polarized light to pass both the formations as it does not see any PBG on the way. In this way, both the polarizations are separated at 90 degrees in a compact area. The proposed device offers a small footprint of ~10.9 μm², low transmission loss of 1.57 dB - 3.5 dB and 0.25 dB - 2 dB for TE and TM-polarized light (for

S, C and L band), high polarization extinction ratio of ~40.5 dB and ~6.5 dB for TM and TE-polarized light which makes it likely to be employed in the on-chip polarization division multiplexing systems for doubling the transmission capacity.

Author Contributions: Conceptualization, M.A.B., N.L.K. and S.N.K.; methodology, M.A.B., N.L.K. and S.N.K.; software, M.A.B., N.L.K. and S.N.K.; validation, M.A.B., N.L.K. and S.N.K.; formal analysis, M.A.B., N.L.K. and S.N.K.; investigation, M.A.B., N.L.K. and S.N.K.; resources, M.A.B., N.L.K. and S.N.K.; data curation, M.A.B., N.L.K. and S.N.K.; writing—original draft preparation, M.A.B., N.L.K. and S.N.K.; writing—review and editing, M.A.B., N.L.K. and S.N.K.; visualization, M.A.B., N.L.K. and S.N.K.; supervision, M.A.B., N.L.K. and S.N.K.; project administration, M.A.B., N.L.K. and S.N.K.; funding acquisition, M.A.B., N.L.K. and S.N.K. All authors have read and agreed to the published version of the manuscript.

Funding: This work was financially supported by the Ministry of Science and Higher Education of the Russian Federation under the Samara National Research University (the scientific state assignment No. 0777-2020-0017) for numerical calculations and under the FSRC "Crystallography and Photonics" of the Russian Academy of Sciences (the state task No. 007-GZ/Ch3363/26) for theoretical research.

Acknowledgements: We acknowledge the contribution of all the authors in completing this work.

Conflicts of Interest: The authors declare no conflict of interest.

References

1. Yablonovitch, E. Inhibited spontaneous emission in solid-state physics and electronics. *Phys. Rev. Lett*. **1987**, 58, 2059.
2. John, S. Strong localization of photons in certain disordered dielectric superlattices. *Phys. Rev. Lett*. **1987**, 58, 2486.
3. Kazanskiy, N.L.; Butt, M.A. One-dimensional photonic crystal waveguide based on the SOI platform for transverse magnetic polarization-maintaining devices. *Photonics Letters of Poland* **2020**, 12, 85-87.
4. Solli, D.R.; McCormick, C.F.; Chiao, R.Y.; Hickmann, J.M. Photonic crystal polarizers and polarizing beam splitters. *Journal of Applied Physics* **2003**, 93, 9429.
5. Morita, Y.; Tsuji, Y.; Hirayama, K. Proposal for a compact resonant-coupling-type polarization splitter based on Photonic Crystal waveguide with absolute Photonic Bandgap. *IEEE Photonics Technology Letters* **2008**, 20, 93-95.
6. Li, X.; Shen, H.; Li, T.; Liu, J.; Huang, X. T-shaped polarization beam splitter based on two-dimensional photonic crystal waveguide structures. *Optical Review* **2016**, 23, 950-954.
7. Chen, C-C.; Chien, H-D.; Luan, P-G. Photonic crystal beam splitters. *Applied Optics* **2004**, 43, 6187-6190.
8. Park, I.; Lee, H-S.; Kim, H-J.; Moon, K-M.; Lee, S-G.; O, B-H.; Park, S-G.; Lee, E-H. Photonic crystal power-splitter based on directional coupling. *Optics Express* **2004**, 12, 3599-3604.
9. Liu, W.; Ma, H.; Walsh, A. Advance in photonic crystal solar cells. *Renewable and sustainable energy reviews* **2019**, 116, 109436.
10. Mohammadi, M.; Moradiani, F.; Olyaee, S.; Seifouri, M. The design and 3D simulation of a new high-speed half adder based on graphene resonators. *Optics & Laser Technology* **2021**, 142, 107280.
11. Parandin, F.; Kamarian, R.; Jomour, M. Optical 1-bit comparator based on two-dimensional photonic crystals. *Applied Optics* **2021**, 60, 2275-2280.
12. Sharifi, H.; Hamidi, S.M.; Navi, K. All-optical photonic crystal logic gates using nonlinear directional coupler. *Photonics and Nanostructures-Fundamentals and applications* **2017**, 27, 55-63.
13. Janfada, M.; Malekmohammad, M.; Soltanolkotabi, M. Design of high-efficiency small-size passive all-optical diodes based on photonic crystal and graphene. *Journal of the Optical Society of America B* **2019**, 36, 1748-1757.
14. Zheng, W. Semiconductor photonic crystal laser. *Chinese Physics B* **2018**, 27, 114211.
15. Najafgholinezhad, S.; Olyaee, S. A photonic crystal biosensor with temperature dependency investigation of micro-cavity resonator. *Optik* **2014**, 125, 6562-6565.
16. Prather, D.W.; Shi, S.; Murakowski, J.; Schneider, G.J.; Sharkawy, A.; Chen, C.; Miao, B.; Martin, R. Self-collimation in photonic crystal structures: a new paradigm for applications and device development. *Journal of Physics D: Applied Physics* **2007**, 40, 2635.
17. J. Witzens, M. Loncar, A. Scherer, *IEEE Journal of Selected Topics in Quantum Electronics* **2002**, 8, 1246.
18. Butt, M.A.; Khonina, S.N.; Kazanskiy, S.N. Recent advances in photonic crystal optical devices: A review. *Optics & Laser Technology* **2021**, 142, 107265.
19. Kazanskiy, N.L.; Khonina, S.N.; Karpeev, S.V.; Porfirev, A.P. Diffractive optical elements for multiplexing structured laser beams. *Quantum Electronics* **2020**, 50, 629.
20. Pauwels, J.; Sande, G. V.D.; Verschaffelt, G. Space division multiplexing in standard multi-mode optical fibers based on speckle pattern classification. *Scientific Reports* **2019**, 9, 17597.
21. Khonina, S.N.; Savelyev, D.A.; Kazanskiy, N.L. Vortex phase elements as detectors of polarization state. Optics Express 2015, 23, 17845-17859.

22. Karpeev, S.V.; Podlipnov, V.V.; Khonina, S.N.; Paranin, V.D.; Reshetnikov, A.S. A foursector polarization converter integrated in a calcite crystal. Computer Optics 2018, 42, 401-407.
23. Khonina, S.N.; Porfirev, A.P.; Karpeev, S.V. Recognition of polarization and phase states of light based on the interaction of nonuniformity polarized laser beams with singular phase structures. Optics Express 2019, 27, 18484-18492.
24. Khonina, S.N.; Ustinov, A.V. Focusing of shifted vortex beams of arbitrary order with different polarization. Optics Communications 2018, 426, 359-365.
25. Dai, D.; Bowers, J.E. Silicon-based on-chip multiplexing technologies and devices for Peta-bit optical interconnects. *Nanophotonics* **2013**, 3, 283-311.
26. Khorin, P.A.; Volotovskiy, S.G.; Khonina, S.N. Optical detection of values of separate aberrations using a multi-channel filter matched with phase Zernike functions. Computer Optics 2021, 45, 525-533.
27. Shechter, R.; Amitai, Y.; Friesem, A.A. Compact wavelength division multiplexers and demultiplexers. *Applied Optics* **2002**, 41, 1256-1261.
28. Morant, M.; Perez, J.; Llorente, R. Polarization Division Multiplexing of OFDM Radio-over-Fiber Signals in Passive Optical Networks. *Advances in Optical Technologies* **2014**, 2014, 269524.
29. Wu, X.; Huang, C.; Xu, K.; Shu, C.; Tsang, H.K. Mode-division multiplexing for silicon photonic network-on-chip. Journal of Lightwave Technology **2017**, 35, 3223-3228.
30. Wang, J.; Chen, P.; Chen, S.; Shi, Y.; Dai, D. Improved 8-channel silicon mode demultiplexer with grating polarizers. *Optics Express* **2014,** 22, 12799-12807.
31. Xiang, L.; Yu, Y.; Qin, Y.; Zou, J.; Zou, B.; Zhang, X. SOI based ultracompact polarization insensitive filter for PDM signal processing. *Optics Letters* **2013**, 38, 2379-2381.
32. Wang, Y.; Zhang, Y.; Jiang, Z.; Deng, W.; Zhou D.; Huang, X.; Yan, Q.; Zhang, J.; Chen, L.; Yu, Y.; Li, X.; Ye, L.; Zhang, X. Ultracompact high-speed polarization division multiplexing optical receiving chip enabled by graphene-on-plasmonic slot waveguide photodetectors. *Advanced Optical Materials* **2021**, 9, 2001215.
33. Goossens, J-W.; Yousefi, M.I.; Jaouen, Y.; Hafermann, H. Polarization-division multiplexing based on the nonlinear Fourier transform. *Optics Express* **2017**, 25, 26437-26452.
34. Melloni, A.; Monguzzi, P.; Costa, R.; Martinelli, M. Design of curved waveguides: the matched bend. *Journal of the Optical Society of America A* **2003**, 20, 130-137.
35. Sarkar, P.; Panda, A.; Palai, G. Analysis of 90^{o} bend photonic crystal waveguide: an application to optical interconnect. *Indian Journal of Physics* **2019**, 93, 1495-1500.
36. Butt, M.A.; Khonina, S.N.; Kazanskiy, N.L. 2D-Photonic crystal heterostructures for the realization of compact photonic devices. *Photonics and Nanostructures-Fundamentals and Applications* **2021**, 44, 100903.
37. Assefa, S.; McNab, S.J.; Vlasov, Y.A. Transmission of slow light through photonic crystal waveguide bends. *Optics Letters* **2006**, 31, 745-747.
38. Sharkawy, A.; Pustai, D.; Shi, S.; Prather, D.W. High transmission through waveguide bends by use of polycrystalline photonic-crystal structures. Optics Letters **2003**, 28, 1197-1199.
39. Chutinan, A.; Noda, S. Highly confined waveguides and waveguide bends in three-dimensional photonic crystal. *Appl. Phys. Lett*. **1999**, 75, 3739-3741.
40. Kim, D.W.; Lee, M.H.; Kim, Y.; Kim, K.H. Ultracompact transverse magnetic mode-pass filter based on one-dimensional photonic crystals with subwavelength structures. Opt. Express 2016, 24, 21560-21565.
41. Sinha, R.K.; Karla, Y. Design of optical waveguide polarizer using photonic band gap. Optics Express 2006, 14, 10790-10794.
42. Yu, T.; Huang, J.; Liu, N.; Yang, J.; Liao, Q.; Jiang, X. Design of a compact polarizing beam splitter based on a photonic crystal ring resonator with a triangular lattice. Applied Optics 2010, 49, 2168-2172.
43. Guan, X.; Chen, P.; Chen, S.; Xu, P.; Shi, Y.; Dai, D. Low-loss ultracompact transverse magnetic-pass polarizer with a silicon subwavelength grating waveguide. Opt. Lett. 2014, 39, 4514-4517.
44. Zabelin, V.; Dunbar, L.A.; Thomas, N.L.; Houdre, R.; Kotlyar, M.V.; Faolain, L.O.; Krauss, T.F. Self-collimating photonic crystal polarization beam splitter. *Optics Letters* **2007,** 32, 530-532.